Reducing charge recombination losses in solid state dye sensitized solar cells: the use of donor–acceptor sensitizer dyes†

Samantha Handa,[a] Helga Wietasch,[b] Mukundan Thelakkat,*[b] James R. Durrant[a] and Saif A. Haque*[a]

Received (in Cambridge, UK) 22nd December 2006, Accepted 23rd February 2007
First published as an Advance Article on the web 3rd April 2007
DOI: 10.1039/b618700e

Herein we report the application of supramolecular dyes to control charge recombination between photo-injected electrons and oxidized hole-transporting material, resulting in an enhancement in the performance of dye sensitized solar cell devices based upon such dyes.

Nanostructured composites of inorganic and organic semiconducting materials are currently attracting extensive interest for a variety of molecular electronic device applications ranging from solar cells, data storage memories and light emitting displays.[1–3] The efficient operation of such devices ultimately depends on the ability to control charge transfer at the device heterojunction. Such dynamics are particularly relevant for the development and subsequent optimization of solid-state dye sensitized nanocrystalline solar cells (DSSC's).[4–7] A typical solid-state DSSC comprises a dye sensitized, mesoporous, nanocrystalline TiO_2 film interpenetrated by an organic semiconductor based hole transporting material (HTM), namely spiro-OMeTAD (2,2-7,7-tetrakis(*N*,*N*-di-*para*-methoxyphenyl-amine 9,9′-spirobifluorene). Solar-light to electrical conversion efficiencies approaching 5%[8] have been reported for such devices, making them an attractive option for low cost photovoltaic energy conversion. The function of the device is based upon a light induced charge separation reaction at the TiO_2/dye/HTM interface. The main charge transfer events taking place at such an interface are shown in Fig. 1. Electron injection from the photo-excited state of the dye molecule into the conduction band of the TiO_2 (Reaction 1) is followed by subsequent regeneration of the dye by hole transfer (Reaction 2) from the dye cation to the HTM. The efficient operation of the DSSC device relies upon the minimization of possible recombination pathways as in Fig. 1 (Steps 3 and 4) occurring at the TiO_2/dye/HTM interface, thereby facilitating efficient charge transport and collection at the device electrodes.

We, and others, have recently been focusing on a range of strategies to control interfacial charge recombination dynamics (Reactions 3 and 4) at such nanostructured inorganic/organic heterojunctions, including the use of mobile lithium ions, insulating metal oxide barrier layers and multilayer organic redox cascades.[9–11] More recently, we have shown that the dynamics of the dye cation–TiO_2 electron recombination (Reaction 3) can be modulated by the use of multifunctional sensitizer dyes that exhibit multi-step electron transfer cascades. More specifically, in previous work, we used $Ru(dcbpy)_3^{2+}$ based dyes in which the bipyridyl ligand was modified by the covalent attachment of triaryl amine based electron donating groups.[12–14] By careful structural control of the electron donating moiety we were able to achieve a remarkably long (4 second) charge separated state lifetime.[15] This retardation in observed kinetics was attributed to an increased physical separation between dye cation and TiO_2 film surface, consistent with a multi-step translation of the oxidizing equivalent "hole" away from the surface. Whilst the application of such dyes to control charge recombination Reaction 3 is well established, the use of such dyes to control the charge recombination between the electron in the TiO_2 and the oxidized HTM (Reaction 4) in solid state DSSC's has received little attention to date.[16,17] This is of particular interest as solid-state DSSC's employing organic HTMs tend to suffer from fast interfacial charge recombination losses relative to liquid electrolyte based devices. These faster charge recombination dynamics have been identified as a key factor limiting the performance of solid-state devices.[18,19] For example, in solid state DSSC's, these faster dynamics limit the diffusion length of photo-generated charges within the device, and therefore limit the maximum device thickness (and hence light absorption) compatible with efficient charge collection. This paper reports

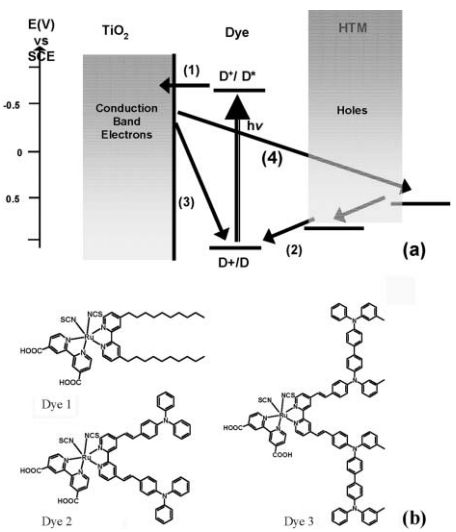

Fig. 1 **a)** Schematic illustration of the charge transfer processes occurring at the dye sensitized nano-crystalline TiO_2/dye/hole transporting material heterojunction. **b)** Also shown are structures of the three dyes employed in this study.

[a]*Centre for Electronic Materials and Devices, Department of Chemistry, Imperial College of Science, Technology and Medicine, London, UK SW7 2AZ. E-mail: s.a.haque@imperial.ac.uk; Fax: +44 (0) 207 5945801; Tel: +44 (0) 207 5945710*
[b]*Applied Functional Polymers, Makromoleculare Chemie 1, Universitat Bayreuth, D-95440, Germany. E-mail: mukundan.thelakkat@uni-bayreuth.de; Fax: 0921/55-3206; Tel: 0921/55-3108*
† Electronic supplementary information (ESI) available: Photovoltaic current–voltage data. See DOI: 10.1039/b618700e

the use of such donor–acceptor super-sensitizer dyes as redox relays in solid state DSSC's. These redox relays allow efficient, multi-step, charge separation whilst increasing the spatial separation of the final charge separated species; photoinjected electrons in the TiO_2 and the oxidized HTM therefore result in a retardation of the charge recombination Reaction 4. These observations show good correlation with the photovoltaic current–voltage characteristics of solid state DSSCs, with the slow charge recombination rate resulting in an increase in the open circuit voltage of up to 50 mV and a 25% improvement in the overall device efficiency.

The chemical structures of the dyes studied herein are shown in Fig. 1b. The dyes are based upon carboxylated Ru(II) polypyridyl chromophores.[15,20–22] Reference dye **1** (commonly referred to as Z907) possesses hydrophobic alkyl side chains (C_9H_{19}) attached on the 4 and 4′ positions of the bipyridyl (bpy) ligand. Dyes **2** and **3** carry aromatic amine electron donating groups attached on the 4 and 4′ positions on the same ligand, namely triphenylamine (TPA) and triphenyldiamine (TPD). Such electron donating groups are known to possess low ionization potentials, which facilitate the formation of cation radicals, thereby allowing multi-step charge transfer to the HTM. In order to obtain evidence for such a multi-step charge transfer cascade within dyes **2** and **3**, we have undertaken density functional theory (DFT) analysis (B3LPY/LANDZ) using Gaussian, to determine the spatial distribution of the highest occupied molecular orbital (HOMO) profile within the dye structure. Fig. 2 compares the HOMO orbital profiles for the three dyes reported herein. The HOMO orbitals for dye **1** are delocalized over the NCS groups. In contrast, in dyes **2** and **3**, the HOMO orbitals are spread over the phenyl amine moieties, thereby resulting in an increased separation of the HOMO orbitals from the TiO_2 surface compared to dye **1**, as desired to achieve charge recombination dynamics. From these data, we estimate the spatial separation (r) of the HOMO orbital of the dye from the metal oxide surface to be 9.8, 10.5 and 11.6 Å for dyes **1**, **2** and **3** respectively.

Dye sensitized nanocrystalline TiO_2 films were prepared as previously described.[23] Where appropriate the spiro-OMeTAD hole transfer material was introduced into the pores of the dye sensitized film by spin coating from a 0.15 M chlorobenzene solution.[17,19] Transient absorption spectroscopy was employed to monitor the charge recombination dynamics (Reactions 3 and 4) following optical excitation of the surface adsorbed dye.[6,15] In the absence of the spiro-OMeTAD, a broad positive absorption band was observed centered around 850 nm (see Fig. 3 inset) for all three dyes and a negative feature at 450 nm for dye **2** and 550 nm for dyes **1** and **3**. These spectral features are assigned, as previously, to the formation of dye cation following photoinduced electron injection (Reaction 1).[15] The charge recombination

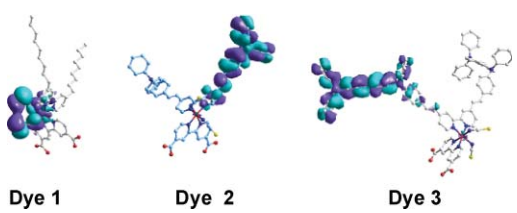

Fig. 2 Graphical representations of the HOMO's of dyes **1**, **2** and **3** studied here as determined from the DFT *ab-initio* calculations reported here.

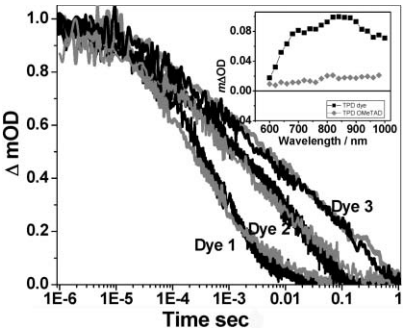

Fig. 3 Transient kinetics observed for TiO_2 electrons with dye cation – Reaction 3 (grey lines) and TiO_2 electrons and OMeTAD cations – Reaction 4 (black lines). Excitation at 520 nm and probed at 800 nm and 1000 nm respectively. Plots are normalized to unity for clearer comparison. Inset: Transient absorption spectra obtained 100 μs after laser excitation of dye **3** sensitized nanocrystalline TiO_2 films in the absence (■) and presence (♦) of HTM spiro-OMeTAD.

kinetics between the injected electrons and dye cations (Reaction 3) were monitored by observing the decay of the 850 nm cation absorption back to ground state. Fig. 3 (black curves) compares the charge recombination dynamics for all three dye–TiO_2 combinations. It is apparent that the recombination dynamics observed for all three dyes differ significantly with dyes **1**, **2**, and **3** exhibiting recombination half-times ($t_{50\%}$) of 220 μs, 1.8 ms and 3 ms respectively. This retardation is consistent with the increased physical separation of the dye cation moiety of the dye from the TiO_2 surface as reported previously.[15] These recombination half times are quantitatively consistent with the distance *versus* recombination half time relationship we have reported previously, based on studies of analogous sensitizer dyes.[15] We note that the recombination dynamics we report here for dyes **1**, **2** and **3** are more dispersive than those we have reported previously. Such dispersive behaviour can be attributed to more inhomogeneous binding orientations of these dyes, resulting from the presence of only two carboxylate binding groups compared to the four carboxylates present in the dyes used in our previous studies.[15]

In the presence of the spiro-OMeTAD a reduction in the photoinduced dye cation signal at 850 nm is observed, as can be seen in Fig. 3 (inset), along with the appearance of a positive feature with an absorption maximum centered at ~520 nm, a spectral feature we have previously assigned to the formation of the OMeTAD radical cation (1). These observations are consistent with the expected hole transfer reaction from the dye cation to the OMeTAD hole transporter (Reaction 2). The yield of hole-transfer (Reaction 2) was determined as previously by comparing the relative amplitudes at 520 nm and 820 nm in the absence and presence of the hole transporting material, both yielding similar results.[24] Measuring the relative amplitudes at 820 nm, the quantum yield for hole-transfer for dyes **1**, **2** and **3** was determined to be 69%, 73% and 79% respectively. The observed hole-transfer from the dye cation to the spiro-OMeTAD is as expected due to the greater ionization potential of the dyes relative to the spiro-OMeTAD (4.9 eV). However, it is apparent that dyes **2** and **3** exhibit superior regeneration efficiency (Reaction 2) compared to dye **1**. Further details await additional studies but these observations appear to be consistent with an improved wetting of the dye sensitized TiO_2 film with the HTM, due to similarity in

This journal is © The Royal Society of Chemistry 2007

Table 1 Summary of device parameters obtained for dye **1** and dye **3**

	V_{oc}/V	J_{sc}/mA cm^{-2}	*FF* %	η %
Dye **1** (device **a**)	0.89	3.9	51	1.8
Dye **3** (device **b**)	0.95	5.0	54	2.6

the chemical nature, and hence polarity between the aryl amine component of the dye and the spiro-OMeTAD.

The dynamics of charge recombination Reaction 4 were determined, as previously, by monitoring the TiO_2 electron absorption at 1000 nm. Fig. 3 (grey lines) shows typical data for dyes **1**, **2** and **3**. It is clear that the recombination dynamics to the dye cation are the same as to spiro-OMeTAD cation. It is also apparent that, depending on which dye is employed, the use of a supersensitizer dye results in a significant retardation of the kinetics relative to the control dye **1**. Moreover the retardation of the recombination dynamics observed for dyes **1**, **2** and **3** mirrors the behaviour observed for the dye cation–electron recombination (Reaction 3), with the recombination dynamics becoming progressively slower as the oxidized moiety 'hole' is shifted away from the surface TiO_2 surface. For dye **1** the oxidized spiro-OMeTAD and therefore the photogenerated holes are likely to remain closer to the TiO_2 surface, leading to a faster charge recombination rate, as observed experimentally. In contrast, for the dyes **2** and **3** the photogenerated holes are expected to reside further away from the surface due the formation of a multi-step charge transfer cascade. Consequently, this would increase the spatial separation between the photogenerated holes in the spiro-OMeTAD and the electrons in the TiO_2, resulting in slower charge recombination dynamics as observed here.

We note that the use of a high dye loading (0.8 ± 0.1 of a monolayer) film was crucial to the observed retardation of the charge recombination (Reaction 4) for dyes **2** and **3**. For example, all TiO_2/dye/OMeTAD samples with low dye loading ($<0.8 \pm 0.1$ of a monolayer) exhibited no significant retardation in the kinetics compared to dye **1**. One possible reason for this could be that the incomplete coverage (<0.8 of a monolayer) of the dye on the nanoporous TiO_2 surface may result in regions of TiO_2 in direct contact with the oxidized spiro-OMeTAD. This is expected to lead to a reduced spatial separation of the photo-generated holes and electrons, resulting in a faster charge recombination rate. These findings further confirm that the supermolecular dyes at complete dye coverage (comparable conditions to device) are functioning as an efficient blocking layer distancing the hole transporting material.

We consider next the photovoltaic performance of the solid-state dye sensitized solar cells based upon such films. Solid-state dye sensitized solar cells were fabricated as previously. Typical values for the photovoltaic parameters (open circuit voltage (V_{oc}), short circuit photocurrent density (J_{sc}), fill factor (*FF*) and the overall energy conversion efficiency (η)) of solar cells employing dye **1** (device **a**) and dye **3** (device **b**) are summarized in Table 1. As expected from the recombination data above, device **b** exhibits improved device performance, with an increase in open circuit voltage of $\sim$50 mV, relative to device **a**. Minimization of interfacial charge recombination losses in device **b** is also evident from the dark-current data for these devices, which addresses the voltage dependence of the recombination between the electrons in the TiO_2 and the oxidized OMeTAD (see ESI†). The reduction in the dark current in device **b** relative to device **a** is consistent with the recombination dynamics discussed above. In addition, we find that device **b** exhibits a significant increase in the short circuit current density (J_{sc}). This observation most probably stems from the superior molar extinction coefficient and the red shift in the absorption spectrum of dye **3** relative to dye **1**.

In summary we have reported the use of supramolecular donor–acceptor dyes to control charge recombination between the photo-injected electrons and oxidized HTM (Reaction 4). The observed retardation in charge recombination rate is consistent with an increased spatial separation of the photogenerated holes and electrons. Solid-state dye sensitized solar cells employing such sensitizers show an improvement in all cell parameters (V_{oc}, J_{sc} and *FF*) and a $\sim$25% enhancement in the overall device performance. The present findings show that the use of multifunctional, supermolecular dyes provides a versatile approach to control interfacial charge transfer and to improve the performance of solid-state dye sensitized solar cells.

This work was funded by the SOHYD EPSRC-ESF project. S. A. H. is a Royal Society University Research Fellow.

Notes and references

1 U. Bach, D. Lupo, P. Comte, J. E. Moser, F. Weissortel, J. Salbeck, H. Spreitzer and M. Gratzel, *Nature*, 1998, **395**(6702), 583.
2 S. Coe, W. K. Woo, M. Bawendi and V. Bulovic, *Nature*, 2002, **420**(6917), 800.
3 W. U. Huynh, J. J. Dittmer and A. P. Alivisatos, *Science*, 2002, **295**(5564), 2425.
4 J. R. Durrant, *J. Photochem. Photobiol., A*, 2002, **148**, 5.
5 S. A. Haque, T. Park, C. Xu, S. Koops, N. Schulte, R. J. Potter, A. B. Holmes and J. R. Durrant, *Adv. Funct. Mater.*, 2004, **14**(5), 435–440.
6 S. A. Haque, Y. Tachibana, R. L. Willis, J. E. Moser, M. Gratzel, D. R. Klug and J. R. Durrant, *J. Phys. Chem. B*, 2000, **104**, 538.
7 J. R. Durrant and S. A. Haque, *Nat. Mater.*, 2003, **2**, 362.
8 M. Gratzel, *J. Photochem. Photobiol., A*, 2004, **164**, 3.
9 T. Park, S. A. Haque, R. J. Potter, A. B. Holmes and J. R. Durrant, *Chem. Commun.*, 2003, **23**, 2878–2879.
10 N. Hirata, J. E. Kroeze, T. Park, D. Jones, S. A. Haque, A. B. Holmes and J. R. Durrant, *Chem. Commun.*, 2006, **5**, 535.
11 E. Palomares, J. N. Clifford, S. A. Haque, T. Lutz and J. R. Durrant, *Chem. Commun.*, 2002, **14**, 1464.
12 K. Peter and M. Thelakkat, *Appl. Phys. A: Mater. Sci. Process.*, 2004, **79**, 65.
13 K. Peter and M. Thelakkat, *Macromolecules*, 2003, **36**, 1779.
14 B. Peng, *Proc. SPIE–Int. Soc. Opt. Eng.*, 2004, **5215**, 60.
15 S. A. Haque, S. Handa, E. Palomares, M. Thelakkat and J. R. Durrant, *Angew. Chem., Int. Ed.*, 2005, **44**, 5740.
16 B. Li, L. Wang, B. Kang, P. Wang and Y. Qiu, *Sol. Energy Mater.*, 2006, **90**, 549.
17 L. Schmidt-Mende, J. E. Kroeze, J. R. Durrant, M. K. Nazeeruddin and M. Gratzel, *Nano Lett.*, 2005, **5**, 1315.
18 J. R. Durrant, S. A. Haque and E. Palomares, *Coord. Chem. Rev.*, 2004, **248**, 1247.
19 J. Kruger, R. Plass, L. Cevey, M. Piccirelli, M. Gratzel and U. Bach, *Appl. Phys. Lett.*, 2001, **79**, 2085.
20 C. Klein, M. K. Nazeeruddin, P. Liska, D. Di Censo, N. Hirata, E. Palomares, J. R. Durrant and M. Gratzel, *Inorg. Chem.*, 2005, **44**, 178.
21 M. K. Nazeeruddin, C. Klein, P. Liska and M. Gratzel, *Coord. Chem. Rev.*, 2005, **249**, 1460.
22 P. Wang, S. M. Zakeeruddin, J. E. Moser, R. Humphry-Baker, P. Comte, V. Aranyos, A. Hagfeldt, M. K. Nazeeruddin and M. Gratzel, *Adv. Mater.*, 2004, **16**, 1806.
23 E. Palomares, J. N. Clifford, S. A. Haque, T. Lutz and J. R. Durrant, *J. Am. Chem. Soc.*, 2003, **125**, 475.
24 S. A. Haque, T. Park, A. B. Holmes and J. R. Durrant, *ChemPhysChem*, 2003, **4**(1), 89–93.